Self-sustained oscillations and chaos in space charge limited currents

Yu. N. Gartstein and P. S. Ramesh
Xerox Corporation, Wilson Center for Research and Technology, 147-59B, 800 Phillips Road, Webster, New York 14580
(Received 7 October 1998; revised manuscript received 24 February 1999)

In kinetic simulations of a flow of charged particles between two parallel plate electrodes, it is found that chaotic responses in space charge limited currents can be induced by a periodically varying applied voltage. [S1063-651X(99)10707-4]

PACS number(s): 05.45.−a, 52.80.Vp

Space charge limited currents (SCLCs) in vacuum tubes are a classical subject with the history going back to the beginning of this century (see, e.g., Refs. [1,2]). Commonly, it is referred to in connection with the famous Langmuir-child $\frac{3}{2}$-power law [1,2] describing a nonlinear current-voltage relation for electrons moving between cathode and anode electrodes. Analysis of current-voltage relations is more involved when electrons have arbitrary initial velocities. Our interest in this topic has been stimulated by problems arising in the context of some modern xerographic technologies. In the process of xerographic development, charged resin microparticles (so-called toners) are ''injected'' from the side of one electrode, a donor, and can be collected on the opposite electrode, a receiver. Although all the physical parameters such as charge and mass of toners or the interelectrode spacing are very different from those occurring in vacuum-tube electronics, the relevant combined quantities can be in the same range where space charge effects are of importance. In this paper we are concerned with a situation where all particles injected at the donor electrode are identical and have nearly equal initial velocities. The idealized mathematical model of such a system was shown to reveal interesting properties. A classical steady-state analysis found multiple types of electrostatic potential distribution in between electrodes [3], and phenomena like a hysteretic response [3,4] and negative resistance [5] were discussed. Later computer simulations demonstrated a dynamical occurrence of the hysteresis. What is more, the system was found to exhibit self-sustained oscillations [6–8]. In the present Report we further emphasize a complex nonlinear-dynamical-system nature of this seemingly simple system by showing that its periodic perturbation can lead to chaotic responses in space charge limited currents.

For clarity, the system under consideration is ''introduced'' in Fig. 1, which shows current-voltage relations between parallel plate electrodes in terms of the transmitted current J as a fraction of the injected current j, as has been calculated in the simulations described below. In case (1) the injected charged particles had zero initial velocities. Curve (1) precisely reproduces the Langmuir-Child law until some applied voltage V_m at which the current becomes supply limited (SLC), $J=j$ [9]. Very different current-voltage relations are represented by curves (2). Here the injected current j was the *same* but all particles had a finite initial velocity corresponding to the kinetic energy $q\phi_0$. (For certainty, the particle charge $q>0$. The applied voltage V is simply the difference of the electrode potentials. See Ref. [9] for other definitions.) A notable feature of current-voltage relation (2) shown with the circular data points is a hysteresis where the system can carry both SCLC and SLC depending on which side the voltage V is approached from. Transitions between these two branches are abrupt when the system jumps from one state to the other [6–8]. Computer simulations showed that no steady state is achieved here in the SCLC regime. What happens instead are self-sustained oscillations that would diminish upon broadening the injection energy distribution [6–8]. Note that shown in Fig. 1 and discussed in Ref. [8] is a hysteresis with respect to a varied applied voltage, while the hysteresis of Refs. [6,7] is that with respect to the injection current variations with the diode being short-circuited.

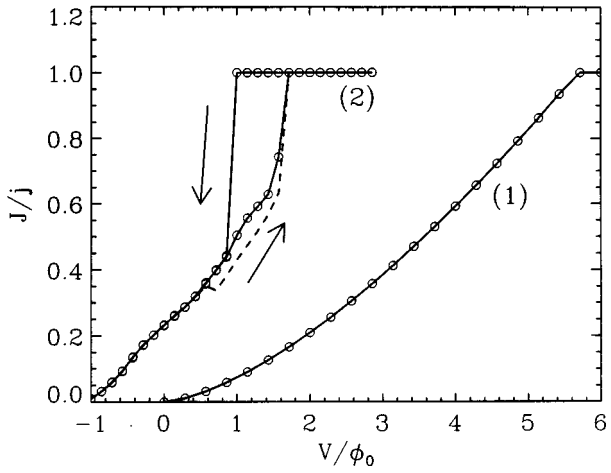

FIG. 1. The transmitted current J as a fraction of the injected j for $P=5.98$ as a function of the applied voltage. Case (1) corresponds to zero injection velocities, in case (2) the injection energy is $q\phi_0$. The circles denote the data points calculated, and the solid lines just connect them. The arrows indicate the direction of the voltage change for the two branches. The dashed line shows the third branch where the voltage was changed from inside that voltage segment starting from the specially prepared state [case (c) in Fig. 2]. Although not shown with the data points, the calculations here were performed also only for the same voltage steps as those connected with the solid lines. In actuality, all the transitions between different branches are abrupt, that is, ''vertical,'' and would happen at some voltage intermediate between the chosen steps.

The results in Fig. 1 have been obtained using a *dynamical* analysis based on the *collisionless* kinetic equation [10]

$$\frac{\partial f}{\partial t}+v\frac{\partial f}{\partial x}+\frac{F}{m}\frac{\partial f}{\partial v}=0, \tag{1}$$

where $f(t,x,v)$ is a time t-dependent particle distribution function in the phase space of the one-dimensional coordinate x and velocity v. The self-consistent force acting on particles is given by $F=-q\partial\phi/\partial x$ with the electrostatic potential ϕ found from Poisson's equation where the particle density $\rho(t,x)=\int_v f(t,x,v)dv$. In the spirit of Liouville's theorem [11], the system has been represented by phase space points whose dynamics is followed according to the self-consistent force [8]. It is instructive to realize that the system under consideration belongs to the class of nonlinear dissipative systems. The nonlinearity here is provided by space charge while the *interaction with the electrodes* provides generalized dissipation. Indeed, consider, e.g., the total ''mass'' in the gap, $M(t)=\int\rho(t,x)dx$. Injection of additional particles would increase this amount (''negative resistance'') while absorption of particles that reach electrodes would reduce the total mass (''positive resistance''). The behavior of the system is significantly affected by the boundary, or dissipation, conditions. The case we are interested in corresponds, on one hand, to the equal energy continuous injection at the donor and, on the other hand, to the reflectionless absorption by the donor and by the receiver of particle that reach them moving from inside the gap. Practically, the shorter the simulation time steps are the closer the approach would be to the continuous injection. A truly continuum system with an infinite number of degrees of freedom is represented therefore by a system with a finite and variable number of degrees of freedom (double the number of the phase space points at a given moment of time). For present results, the time steps have been about 0.008 of the time of flight $\tau_f=L/v_0$where v_0 is the initial velocity.

The hysteretic current-voltage relation (2) represented with circles in Fig. 1 is a result of successive change of the applied voltage by small portions as indicated by the data points and, after the transients die off, of collecting (averaging) the current delivered to the receiver over some fixed period of time. The hysteresis reflects some ''memory'' in the system through the state of the cloud of charged particles in the gap between electrodes induced at earlier times. To illustrate the nonaveraged temporal dynamics, Fig. 2 displays its projection, at $V/\phi_0=1$, onto the plane of two ''macroscopic'' variables M and X_c where the relative position of the center of mass $X_c(t)=(ML)^{-1}\int x\rho(t,x)dx$.Point (a) (for clarity surrounded by a circle) corresponds to the SLC part of the current-voltage relation, with the variables obviously constant for this steady state. Various phase trajectories would approach point (a) [8] in a way characteristic of stable nodes [12,13]. The SCLC counterpart of the current-voltage relation reveals, however, an oscillatory dynamics appearing as limit cycle (b) in Fig. 2 [8,14]. The abrupt transitions between SLC and SCLC in Fig. 1 correspond to the node or limit cycle losing their respective stability. The history leading to state (b) is determined by a slow ascent along the SCLC curve in Fig. 1. Surprisingly, as was found in Ref. [6], some other history routes can lead to another, at least one more stable limit cycle [15] state of our system at the same voltage. The dynamics of this state is shown by curves (c) in Fig. 2. As compared with state (b), state (c) exhibits higher frequency smaller amplitude oscillations The transmitted current J/j for states (a), (b), and (c) at this applied voltage, after averaging over about $47.8\tau_f$, turns out to be 1, 0.51, and 0.43, respectively. When the applied voltage changes by small portions in both directions starting from state (c), the system responds with the current-voltage relations shown by the dashed line in Fig. 1. It jumps to the SCLC or SLC states at the lower and upper ends of this dashed segment. In other words, for a range of applied constant voltages, the system described by Eq. (1) with our boundary conditions can be at least in three different stable states carrying three different currents.

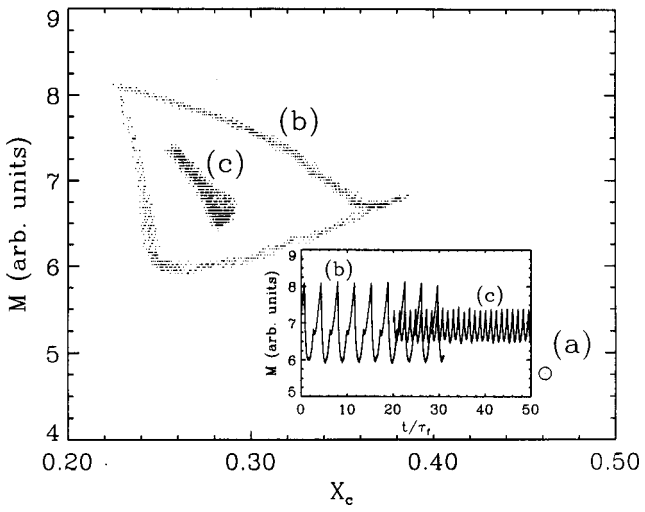

FIG. 2. The long-time phase portraits of the system dynamics in the plane of the cloud total mass vs the relative position of the cloud. Cases (a)–(c) correspond to different stable solutions. The applied voltage $V/\phi_0=1$, $P=5.98$, and the injection energy is $q\phi_0$. The inset shows the temporal evolution of the cloud total mass for oscillating solutions where the time is measured in units of time of flight.

It is known that forced self-oscillatory systems can reveal different types of behavior such as entrainment of frequency and almost periodic oscillations [13]. However, the existence of different stable states of the unperturbed system in the vicinity of each other suggests the possibility of even more complex dynamics of the forced system when, e.g., the latter would move across the regions of the phase space that belonged to different unperturbed domains of attraction [16,17]. We will now study the response of our system to a periodic variation of the applied voltage,

$$V(t)=V_1+V_2\cos(\omega_{\mathrm{driv}}t). \tag{2}$$

The phase portraits shown in Fig. 3 have been obtained for the case of $V_1/\phi_0=1, V_2/\phi_0=0.64$, and the driving force period $T_{\mathrm{per}}/\tau_f=2.39$. Limit cycle (a) in Fig. 3 originates from a sinusoidal response of the system in the SLC regime (in fact, here the amplitude V_2 is insufficient to break the current flow and the injected current is all collected). When originated from the SCLC regime, however, the response

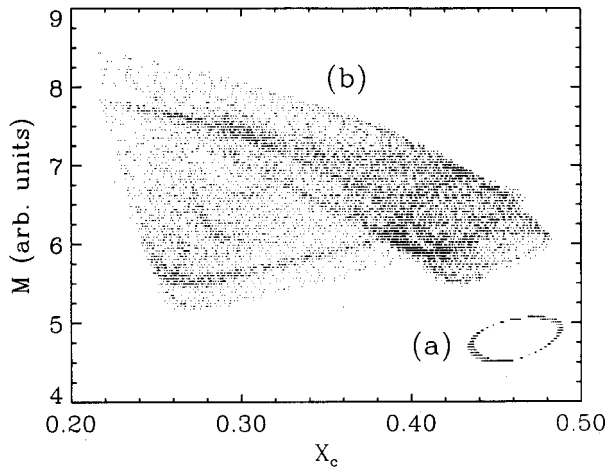

FIG. 3. The long-time phase portraits of the system periodically driven as described in the text. Regime (a) corresponds to the SCL-originated solution while (b) originates in the SCLC. $P=5.98$ and the injection energy is $q\phi_0$.

forms quite an entangled figure (b) in Fig. 3, reminiscent of strange attractors [12,18]. Both temporal variations of M and of the current transmitted per driving period also appear chaotic. To get a better idea of the degree of irregularity of the dynamics associated with case (b), we simulated it over 1000 driving periods and calculated the power spectrum of the variations of $M(t)$, which is shown in Fig. 4. Besides the pronounced peak corresponding to the driving frequency, the spectrum exhibits the features characteristic of chaotic motion [17–19]. The spectrum is practically continuous and has substantial power in the low frequency region. As is known, an almost periodic motion would have an essentially discrete spectrum [17–20]. A crucial feature of the motion on the strange attractor is its sensitive dependence on initial conditions. Figure 5 illustrates such a dependence for our system.

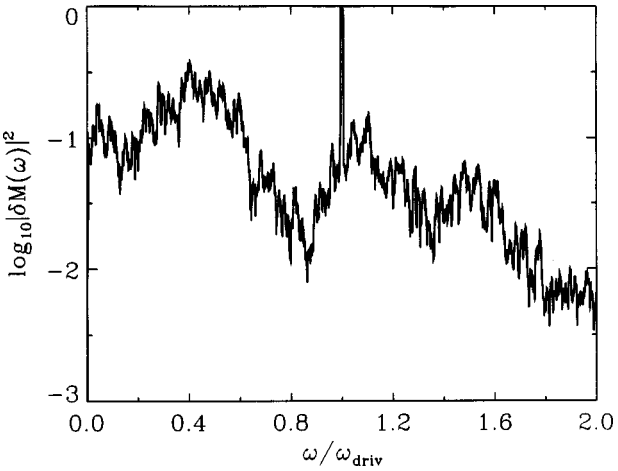

FIG. 4. The power spectrum of the cloud mass variations in the periodically forced system as exemplified by phase portrait (b) in Fig. 3. Here the simulations ran over 1000 external force periods, after which the overall average was determined and variations $\delta M(t)$ calculated with respect to that average. $\delta M(\omega)$ are Fourier components of those variations. For clarity, the actual data were additionally box averaged over frequency intervals of $\delta\omega = 0.01\omega_{\rm driv}$.

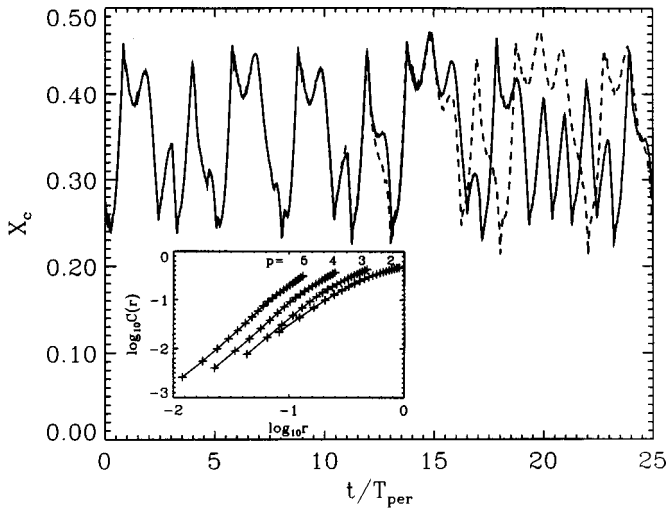

FIG. 5. An illustration of the divergence of two nearby trajectories shown with solid and dashed lines, respectively. At time $t=0$, a tiny detuning of 10^{-8} of the period was introduced in the phase of the driving force. The inset shows a log-log plot of the normalized number of pairs of points on the reconstructed trajectory within a given distance in embedding spaces of different dimensions p. The leveled off slope at higher p gives the correlation dimension of the attractor. For clarity, the curves at different p were displaced from each other along the x axis.

Since we are dealing with a nonautonoumous system, for full characterization of its state, time t must also be specified [12]. Figure 5 compares the time dependence of two trajectories (in terms of the macroscopic coordinate X_c) whose difference was caused by a tiny detuning of the phase of the driving force at time $t=0$, corresponding to the time shift $t \rightarrow t+10^{-8}T_{\rm per}$ in Eq. (2). The system was driven for a long time for transients to decay by $t=0$. Evidently the trajectories ''completely'' diverge within about 20 periods of the driving force. We observed a similar picture for numerous other examples and had all indications of the positive largest Liapunov exponent [12,18,20], although we could not reliably quantify it. For a more quantitative characterization of the attractor, we chose, as is frequently convenient, to determine its correlation dimension [12,18,20]. As described in those references, we used the attractor reconstruction technique, analyzing trajectories in spaces of a series of delayed coordinates $(X_c(t), X_c(t+\tau), \ldots, X_c[t+(p-1)\tau])$. The delay time τ and embedding dimension p were varied. The inset in Fig. 5 shows a log-log plot of the normalized number $C(r)$ of pairs of trajectory points within distance r from each other in the embedding spaces of various p [20]. For this plot, 2000 trajectory points were used with $\tau=0.2T_{\rm per}$. Apparently, the slope of log-log graphs quickly levels off at higher p, yielding the attractor correlation dimension of about (somewhat larger than) 2. This again strongly indicated ''low-dimensional deterministic chaos'' in our system rather than noise that could be caused by a large number of independent degrees of freedom [12,20]. Changing the parameters of the driving force in Eq. (2) we have been able to observe different degrees of irregularity in the dynamics. Higher amplitudes V_2 can cause switching to the SLC re-

gime. In this report we do not pursue a quantitative study of the motion dependence on the parameters of the driving force.

In conclusion, we have further demonstrated that such a seemingly simple system consisting of one type of charge carriers executing flights in the gap between two electrodes can exhibit many fascinating features of nonlinear dissipative dynamical systems. In addition to earlier known self-sustained oscillations and hysteresis, chaotic responses have now been found to be induced by a periodic applied force.

[1] I. Langmuir and K. T. Compton, Rev. Mod. Phys. **3**, 191 (1931).

[2] J. Millman, *Vacuum-tube and Semiconductor Electronics* (McGraw-Hill, New York, 1958).

[3] See, e.g., C. E. Fay, A. L. Samuel, and W. Shockley, Bell Syst. Tech. J. **17**, 49 (1938), and references therein, and an extensive bibliography in Ref. [7].

[4] E. W. B. Gill, Philos. Mag. **49**, 993 (1925).

[5] L. Tonks, Phys. Rev. **30**, 501 (1927).

[6] C. K. Birdsall and W. B. Bridges, J. Appl. Phys. **32**, 2611 (1961); W. B. Bridges and C. K. Birdsall, *ibid.* **34**, 29461 (1963).

[7] C. K. Birdsall and W. B. Bridges, *Electron Dynamics of Diode Regions* (Academic, New York, 1966).

[8] Yu. N. Gartstein and P. S. Ramesh, J. Appl. Phys. **83**, 2958 (1998); **84**, 1158 (1998).

[9] If ϕ_0 is used as an appropriate voltage scale, then the magnitude of space charge effects is related to the parameter $P = jL^2(qm/2)^{1/2}/\epsilon\phi_0^{3/2}$ where L is the distance between the electrodes, m the particle mass, and ϵ the permeability of the vacuum (or another medium between electrodes). In simulations for Fig. 1, $P = 5.98$. From the Langmuir-Child law, the voltage for the onset of SLC on curve (1) $V_m/\phi_0 = (9P/4)^{2/3} = 5.67$, as indeed is found in the simulations.

[10] E. M. Lifshitz and L. P. Pitaevskii, *Physical Kinetics* (Pergamon, Oxford, 1981).

[11] L. D. Landau and E. M. Lifshitz, *Statistical Physics, Part 1* (Pergamon, Oxford, 1980).

[12] See, e.g., S. H. Strogatz, *Nonlinear Dynamics and Chaos* (Addison-Wiley, Reading, MA, 1995).

[13] C. Hayashi, *Nonlinear Oscillations in Physical Systems* (Princeton University Press, Princeton, NJ, 1985).

[14] As was found in our simulations [8], the oscillations of the charged cloud in the gap persist even at such negative voltages where no net current flows through the system. Only at some negative enough voltage, the oscillations cease to exist and the dynamic simulation picture would correspond to the one expected from the steady-state classic analysis. This transition voltage point signifies a Hopf limit cycle bifurcation [12].

[15] The finite thickness of limit cycles in Fig. 2 is due to finite time steps in our simulations. A better resolution is achievable when the time steps are decreased.

[16] F. C. Hoppensteadt, *Analysis and Simulation of Chaotic Systems* (Springer, New York, 1993).

[17] J. Guckenheimer and P. Holmes, *Nonlinear Oscillations, Dynamical Systems, and Bifurcations of Vector Fields* (Springer, New York, 1983).

[18] A. J. Lichtenberg and M. A. Lieberman, *Regular and Chaotic Dynamics* (Springer, New York, 1992).

[19] G. M. Zaslavskii and R. Z. Sagdeev, *Introduction to Nonlinear Physics* (Nauka, Moscow, 1988).

[20] P. Bergé, Y. Pomeau, and C. Vidal, *Order Within Chaos* (Wiley, New York, 1984).